

# **EFFECT OF RESISTANCE SPOT WELDING PARAMETERS ON COPPER AND BRASS**

**by**

**NURIHAL HANIM BT MAT SAAD**

**Thesis submitted in fulfilment of the requirements for the degree of  
Master of Science**

**APRIL 2012**

## **DECLARATION**

**I hereby declare that I have conducted, completed the research work and written the thesis entitled “Effect of Resistance Spot Welding Parameter on Copper and Brass”. I also declare that it has not been previously submitted for award for any degree or diploma or other similar title for any other examining body or University.**

**Name of student: NURIHAL HANIM BT MAT SAAD**

**Signature:**

**Date: 02<sup>nd</sup> April 2012**

**Witness by**

**Supervisor: ASSOC. PROF. AHMAD BADRI BIN ISMAIL    Signature:**

**Date: 02<sup>nd</sup> April 2012**

## ACKNOWLEDGEMENTS

I would like to express my deeply sincere appreciate to my academic supervisor, Assoc. Prof. Ahmad Badri Bin Ismail for his time, guidance, support and assistance in this endeavour, who assisted me to handle all the experimental problems, stimulated discussions on various aspects of my research and provided a lot of valuable information. His knowledge and guidance encouraged me through the journey of this research. I also would like to thank USM's technician for easy access to the facilities in the laboratories and welding facilities.

I am also grateful to thank the USM's Research Creativity and Management Office (RCMO) for Research Intensive Grant for providing financial support (Grant No: 305/PBAHAN/6013351). I also grateful for the financial support by Ministry of Science, Technology & Innovation (MOSTI) for fellowship under National Science Fellowship (NSF), (308.AIPS.415501) scheme.

This research cannot be accomplished without many nice people. I would like to thank my family and friends for giving me support through the good and bad times. With the power of their love, I never give up on the long way to achieve my dream even when I face those tough difficulties and challenges. Especially thanks to my loved ones Wan Mohd Hafez, without his support, encouragement and sacrifice I could have not completed this research and I will always appreciate his understanding of times when research consumed my days and nights and also to my son, Wan Adeeb Akasyah who continually brings love and laughter into my world and keeps life in perspective.

## TABLES OF CONTENTS

DECLARATION.....	ii
ACKNOWLEDGEMENT.....	iii
TABLE OF CONTENTS.....	iv
LIST OF TABLES.....	viii
LIST OF FIGURES.....	x
LIST OF ABBREVIATIONS.....	xviii
LIST OF SYMBOLS.....	xix
ABSTRAK.....	xx
ABSTRACT.....	xxii

### CHAPTER 1 – INTRODUCTION

1.1 Resistance spot welding in general.....	1
1.2 Problem statement.....	4
1.3 Research objective.....	6
1.4 Scopes.....	6

### CHAPTER 2 – LITERATURE REVIEW

2.1 Resistance spot welding (RSW).....	8
2.2 Principle of operation resistance spot welding.....	9
2.2.1 Welding current.....	10
2.2.2 Welding force (electrode force).....	12
2.2.3 Welding time (welding cycles).....	12
2.3 Properties and characteristics of copper and copper alloys.....	14

2.3.1	Copper.....	15
2.3.2	Brass (Cu-Zn) alloy.....	16
2.3.2.1	Structure with Cu-Zn phase diagram.....	17
2.3.2.2	Phase transformation.....	19
2.4	Nugget formation and their characteristics.....	21
2.5	Surface conditions.....	26
2.6	Studies of spot weldability.....	27
2.7	Mechanical performance and microstructure.....	29
2.7.1	Peel off behaviour.....	29
2.7.2	Tensile properties.....	31
2.7.3	Hardness.....	33

## CHAPTER 3 – MATERIALS AND METHODS

3.1	Introduction.....	36
3.2	Raw materials description.....	36
3.3	Specimens.....	37
3.4	Parameter used in the spot welding.....	38
3.5	Micro spot welder machine.....	40
3.6	Copper electrode.....	41
3.7	Mechanical properties evaluation.....	42
3.7.1	Peel off test.....	42
3.7.2	Tensile test.....	44
3.7.3	Hardness testing.....	45
3.8	Microstructural characterization.....	47

## CHAPTER 4 – RESULTS AND DISCUSSION

4.1	Parameter optimization and mechanical properties.....	50
4.1.1	Peel off behaviour.....	50
4.1.1.1	Nugget diameter measurement.....	59
4.1.1.2	Effect of welding current and applied loads on nugget diameter.....	60
4.1.1.3	Porosity.....	64
4.1.2	Tensile properties.....	68
4.1.2.1	Fracture surface.....	73
4.1.3	Hardness profile.....	77
4.2	Metallographic and microstructures analysis of spot welded joint.....	87
4.2.1	Effect of deformation, varied welding current and applied loads on welded joints.....	88
4.2.1.1	Fusion area of copper joints.....	88
4.2.1.2	Heat affected zone (HAZ) area.....	92
4.2.1.3	Nugget growth.....	95
4.2.1.4	Fusion area of brass joints.....	98
4.2.1.5	Heat affected zone (HAZ) area.....	102
4.2.1.6	Nugget growth.....	104
4.2.2	Porosity.....	107
4.2.3	Morphology of weld nugget by EDX analysis.....	109

## CHAPTER 5 –CONCLUSIONS

5.1	Conclusion.....	113
5.2	Recommendations.....	115

REFERENCES.....	116
-----------------	-----

## APPENDICES

### APENDIX A

## LIST OF TABLES

Table 2.1	Welding current (kA) for 0.4 mm diameter nugget, WME and ESS	11
Table 2.2	Copper and copper alloys are classified according to a designation system administered by the Copper Development Association (CDA)	15
Table 2.3	Table of further changes in percentage composition of copper and zinc	18
Table 3.1	Physical properties of raw materials	36
Table 3.2	Parameters used for each specimen at different stage of welding current and applied loads	38
Table 3.3	Table of composition and concentration of ferric chloride etchant	47
Table 4.1	Optical micrograph of fusion area under various welding conditions of copper joints	53
Table 4.2	Optical micrograph of fusion area under various welding conditions of brass joints	55
Table 4.3	Nugget diameter measurements of copper and brass joints	58
Table 4.4	Optical micrographs of fracture surface after tensile test of copper joints under various welding conditions	73
Table 4.5	Optical micrographs of fracture surface after tensile test of brass joints under various welding conditions	74



Table 4.6	Variation of OM micrographs showing the grain pattern of HAZ area of copper joints when welded under various welding conditions, etched for 20 sec. in alcoholic ferric chloride	92
Table 4.7	Variation of OM micrographs showing the larger grains in the weld nugget of copper joints when welded under various welding conditions, etched for 20 sec. in alcoholic ferric chloride	97
Table 4.8	Variation of OM micrographs showing grain structures in the weld nugget of brass joints when welded under various welding conditions, etched for 20 sec. in alcoholic ferric chloride	105
Table 4.9	Variation of SEM micrographs showing the pores in fusion area of brass joints when welded under various welding conditions, etched for 20 sec. in alcoholic ferric chloride	109

## LIST OF FIGURES

Figure 1.1	Typical spot welding cycle	2
Figure 1.2	Schematic representations of the whole experimental procedures	7
Figure 2.1	Schematic figures of (a) micro spot welder machines and (b) the spot weld illustration	9
Figure 2.2	Four stage of spot welding process and weld nugget formation	13
Figure 2.3	Schematic figure of constitutional phase diagram of the Cu-Zn alloy	18
Figure 2.4	Classic microstructure of peritectic alloy, showing rim of $\beta$ -phase separating primary $\alpha$ -phase from (darker) former liquid phase, in Cu-20wt-% Sn	19
Figure 2.5	Example of phase diagram with peritectic transformation	20
Figure 2.6	Micrograph of the spot welded region, (a) weld nugget, (b) heat affected zone (HAZ) and (c) base metal	21
Figure 2.7	Temperature-time curves representing typical thermal cycles experienced in the HAZ of a weld	22
Figure 2.8	Samples, welded in atmosphere and then cooled in atmosphere, show microstructures of weld nugget coarsening by increasing weld current from (a) 4 kA to (b) 7 kA and (c) 9 kA	23

Figure 2.9	Typical micrographs illustrating the location of weld nugget after (a) 9 cycles of current flow in the uncoated stack with an electrode force of 2.1 kN, (b) 10 cycles of current flow in the coated stack with an electrode force of 2.1 kN, and (c) 16 cycles of current flow in the coated stack with an electrode force of 6.0 kN	24
Figure 2.10	Weld nugget growth curve and weldability range	25
Figure 2.11	(a) Effect of electrode force on contact radius and (b) effect of electrode on the size of formed nugget	26
Figure 2.12	(a) Peel force, (b) nugget diameter versus welding current using different electrodes (Class 2 and Class 14), and their fracture surface when using (c) Class 2 and (d) Class 14 for brass joints	29
Figure 2.13	(a) Peel force, (b) nugget diameter versus welding current using different electrodes (Class 2 and Class 14), and their fracture surface when using (c) Class 2 and (d) Class 14 for copper joints	30
Figure 2.14	Effect of welding current on tensile-shear strength of weld joints	32
Figure 2.15	The maximum fracture load versus the welding current in the tensile shear tests	33
Figure 2.16	Micro-hardness distribution in welded joint, (a) the micro-hardness test plan and (b) hardness distribution along line 1 in (a)	34
Figure 2.17	Graphs of the microhardness distribution across weld nugget (a) 2.50 kA, (b) 3.75 kA, (c) 5.00 kA and (d) 6.25 kA	35

Figure 3.1	Dimension for spot welds operation, (a) top view and (b) side view	38
Figure 3.2	SEIWA micro spot welder machine and its accessories	41
Figure 3.3	Copper electrodes	41
Figure 3.4	Schematic figure of nugget diameter measurement on welded joints after peel off test, (a) outside area and (b) inside area	43
Figure 3.5	Schematic figure of the setup for tensile test specimen	44
Figure 3.6	Schematic figures to measure the nugget diameter and spot welded area, A	45
Figure 3.7	Vickers hardness test uses a square-base diamond pyramid as the indenter with an angle of $136^\circ$ opposite faces	46
Figure 3.8	Schematic of micro Vickers hardness shows the values of d1 and d2	46
Figure 4.1	Schematic figures showing joint failure modes during peel off test, (a) failure along interface, (b) failure through nugget and (c) failure as a button pullout	51
Figure 4.2 (a)	Schematic figure showing of interface failure when using 5.50 kA weld current of copper joint	52
Figure 4.2 (b)	Schematic figure showing the failure through weld nugget when using 6.00 kA and 6.50 kA weld current of copper joint	52
Figure 4.3	Schematic figures showing the failure through weld nugget when using 5.50 kA, 6.00 kA and 6.50 kA weld current of brass joint	53

Figure 4.4	Migration of oxygen occurs between two sheets when welding process to form oxides on nugget joined using 5.50 kA weld current under 60 N loads	55
Figure 4.5	Example optical micrograph of splashing surface of brass joint	57
Figure 4.6	Surface cracking in the nugget area when using 5.50 kA weld current under 60 N loads	58
Figure 4.7	(a) Effect of varied applied loads on nugget diameter, (b) effect of varied welding current on nugget diameter for copper joints	61
Figure 4.8	(a) Effect of varied applied loads on nugget diameter, (b) effect of varied welding current on nugget diameter for brass joints	62
Figure 4.9	Effect of weld porosity under different applied loads of copper joints under, (a) 60 N, (b) 65 N, (c) 70 N and (d) 75 N loads	65
Figure 4.10	Optical micrographs shows an example of some pores and excess penetration in fusion area of brass joints, (a) 5.50 kA, (b) 6.00 kA and (c) 6.50 kA weld current under 75 N loads	66
Figure 4.11	Maximum fracture loads versus the welding current for copper joints	69
Figure 4.12	Effect of applied load on tensile-shear strengths of copper joints for different welding current	70
Figure 4.13	Maximum fracture loads versus the welding current for brass joints	71

Figure 4.14	Effect of applied load on tensile-shear strengths of brass joints for different welding current	72
Figure 4.15	Typical loads versus displacement curves with their corresponding failure mode in the tensile-shear testing for copper joints	76
Figure 4.16	Typical loads versus displacement curves with their corresponding failure mode in the tensile-shear testing for brass joints	76
Figure 4.17	Vickers hardness number were taken along the centreline on the cross-section of welds under different applied loads and weld current for copper joints, (a) $I = 8.00$ kA, (b) $I = 8.50$ kA and (c) $I = 8.90$ kA	79
Figure 4.18	Variation of OM microstructures showing larger grains in the weld nugget of copper joints, (a) $I = 8.00$ kA, (b) $I = 8.50$ kA and (c) $I = 8.90$ kA, etched for 20 sec. in alcoholic ferric chloride	82
Figure 4.19	Vickers hardness number were taken along the centreline on the cross-section of welds under different applied loads and weld current for brass joints, (a) $I = 8.00$ kA, (b) $I = 8.50$ kA and (c) $I = 8.90$ kA	83
Figure 4.20	Variation of SEM microstructures showing smaller grains in the weld nugget of brass joints, (a) $I = 8.00$ kA, (b) $I = 8.50$ kA and (c) $I = 8.90$ kA, etched for 20 sec. in alcoholic ferric chloride	86
Figure 4.21	Optical micrograph shows an example of fusion area of brass joint, etched for 20 sec. in alcoholic ferric chloride	87

Figure 4.22	Microstructural changes from the base metal to the weld nugget of copper joints via OM observation, $I = 8.00$ kA, $F = 65$ N, (a) base metal, (b) HAZ area, (c) nugget area, (d) transition area between nugget and HAZ and (e) an overall view of the fusion zone, etched for 20 sec. in alcoholic ferric chloride	89
Figure 4.23	Microstructural changes from the base metal to the weld nugget of copper joints via OM observation, $I = 8.50$ kA, $F = 65$ N, (a) base metal, (b) HAZ area, (c) nugget area, (d) transition area between nugget and HAZ and (e) an overall view of the fusion zone, etched for 20 sec. in alcoholic ferric chloride	90
Figure 4.24	Microstructural changes from the base metal to the weld nugget of copper joints via OM observation, $I = 8.90$ kA, $F = 65$ N, (a) base metal, (b) HAZ area, (c) nugget area, (d) transition area between nugget and HAZ and (e) an overall view of the fusion zone, etched for 20 sec. in alcoholic ferric chloride	91
Figure 4.25	OM micrograph showing $\alpha$ -phase (light) and $\beta$ -phase (dark) of copper joints at 8.00 kA weld current under 65 N loads	92
Figure 4.26	OM micrographs showing the, (a) twin lamellar and (b) lamellar structure for each grains in HAZ area for copper joints	95
Figure 4.27	OM micrographs showing the form grains to be elongated start at the centre of weld nugget of copper joints at 8.00 kA weld current under 65 N loads	96

Figure 4.28	OM micrographs showing the variety shape of copper joints joints, (a) flower-shape and (b) heart-shape, etched for 20 sec. in alcoholic ferric chloride	98
Figure 4.29	Microstructural changes from the base metal to the centre of the of the weld nugget of brass joints via OM observation, $I = 8.00$ kA, $F = 65$ N (a) base metal, (b) HAZ area, (c) nugget area, (d) transition area between nugget, HAZ and base metal and (e) an overall view of the fusion zone, etched for 20 sec. in alcoholic ferric chloride	99
Figure 4.30	Microstructural changes from the base metal to the centre of the of the weld nugget of brass joints via OM observation, $I = 8.50$ kA, $F = 65$ N (a) base metal, (b) HAZ area, (c) nugget area, (d) transition area between nugget, HAZ and base metal and (e) an overall view of the fusion zone, etched for 20 sec. in alcoholic ferric chloride	100
Figure 4.31	Microstructural changes from the base metal to the centre of the of the weld nugget of brass joints via OM observation, $I = 8.90$ kA, $F = 65$ N (a) base metal, (b) HAZ area, (c) nugget area, (d) transition area between nugget, HAZ and base metal and (e) an overall view of the fusion zone, etched for 20 sec. in alcoholic ferric chloride	101
Figure 4.32	SEM micrograph showing the $\alpha$ -phase and $\beta$ -phase in HAZ area of brass joint, etched for 20 sec. in alcoholic ferric chloride	102
Figure 4.33	Schematic peritectic phase diagram showing composition of liquid, $C_L$ and primary phase, $C_\alpha$ , which react to form peritectic $\beta$ -phase	103



Figure 4.34	SEM micrographs showing the weld area, (a) transition area between base metal, HAZ and nugget, (b) transition area between HAZ and nugget of brass joints	106
Figure 4.35	EDX analysis, (a) Surface morphology of copper base metal, (b) microanalysis trace from $\alpha$ -phase area, (c) $\beta$ -phase area and (d) $\alpha$ -phase area of copper weld nugget	110
Figure 4.36	EDX analysis, (a) Surface morphology of brass weld nugget, (b) microanalysis trace from $\beta$ -phase area and (e) $\alpha$ -phase area	112

## LIST OF ABBREVIATIONS

RSW	:	Resistance spot welding
SSRSW	:	Small-scale resistance spot welding
ECAP	:	Equal channel angular pressing
USA	:	United States of America
CDA	:	Copper Development Association
WME	:	Weld metal expulsion
ESS	:	Electrode-sheet sticking
HSLA	:	High-strength low-alloy
BM	:	Base metal
HAZ	:	Heat affected zone
FCC	:	Face centered-cubic
BCC	:	Base centered-cubic
SEM	:	Scanning electron microscope
EDX/EDS	:	Energy Dispersive X-Ray Spectroscopy
UTS	:	Ultimate tensile strength
HV	:	Vickers hardness
FeCl <sub>3</sub>	:	Ferric chloride
HCl	:	Hydrochloric acid
PVC	:	Polyvinyl chloride pipe
Cu-Zn	:	Brass (copper-zinc) alloy
AC	:	Alternate current
DC	:	Direct current

## LIST OF SYMBOLS

Q	:	Heat
I	:	Current
R	:	Resistance; Resistivity
t	:	Time; Thickness
E	:	Voltage drop across the electrodes
Hz	:	Hertz
%	:	Percent
°C	:	Degree celsius
$\sigma$	:	Shear stress
$\alpha$	:	Alpha
$\beta$	:	Beta
A	:	Area
N	:	Newton
F	:	Force
kgf	:	Kilogram-force
nm	:	Nanometre
ms	:	Millisecond
mm	:	millimetres
kA	:	Kilo amperes
GPa	:	Gigapascal
$\mu\text{m}$	:	Micrometre
Amps	:	Amperes

# **KESAN PEMBOLEHUBAH KIMPALAN RINTANGAN BINTIK TERHADAP KUPRUM DAN LOYANG**

## **ABSTRAK**

Kimpalan rintangan bintik adalah kaedah biasa yang digunakan untuk kimpalan logam. Kebanyakan kajian dalam teknik ini hanya tertumpu kepada bahan-bahan terpilih dan hanya sedikit maklumat boleh didapati mengenai tindakbalas dan tingkah laku kuprum dan aloi kuprum. Oleh itu, kajian ini bertujuan untuk mengkaji kesan pembolehubah kimpalan rintangan bintik ke atas kuprum dan aloi loyang. Kuprum dan loyang yang dikimpal melalui teknik kimpalan rintangan bintik di bawah perbezaan arus kimpalan dan tekanan beban telah dikaji. Pengukuran nuget menunjukkan pengaruh beban (60 N, 65 N, 70 N dan 75 N) dan arus kimpalan (5.50 kA, 6.00 kA dan 6.50 kA) pada kedua-dua kawasan pelakuran dan keliangan dalaman. Diameter nuget meningkat pada kadar arus kimpalan rendah dan tinggi, tetapi terhad kepada nilai maksimum pada peringkat pertengahan arus kimpalan. Di samping itu, penyambungan kuprum menunjukkan pembentukan oksida dan retak berlaku, manakala penyambungan loyang menunjukkan lebih pembentukan liang dan penembusan yang berlebihan di kawasan pelakuran. Oleh itu, arus kimpalan ditingkatkan kepada 8.00 kA, 8.50 kA dan 8.90 kA, manakala pembolehubah beban kenaan adalah malar pada 60 N, 65 N, 70 N dan 75 N yang diambil sebagai nilai optimum untuk memperbaiki penyambungan kimpalan. Sifat-sifat mekanikal dan mikrostruktur kimpalan kuprum dan loyang juga diperincikan. Spesimen pada arus kimpalan tinggi menghasilkan lebih tinggi hasil kekuatan tegangan ricih daripada arus kimpalan rendah. Mod kegagalan diperincikan dengan pemerhatian permukaan patah kimpal. Korelasi antara logam asas dan kekerasan zon pelakuran dihasilkan.

Penyambungan loyang memberikan nilai kekerasan yang tertinggi pada nugget kimpal kerana penghalusan struktur bijian dan ini diikuti oleh HAZ dan asas logam asal. Manakala penyambungan kuprum menunjukkan nugget kimpal memberikan nilai kekerasan terendah daripada logam asas asal disebabkan pelembutan penyepuhlindapan dominan menyebabkan pengasaran struktur bijian.

# **EFFECT OF RESISTANCE SPOT WELDING PARAMETERS ON COPPER AND BRASS**

## **ABSTRACT**

Resistance spot welding is the most commonly used method for joining sheet metals. Most studies in this technique were focus on selected materials and little information is available regarding the response and behaviour of copper and copper alloy. Thus, in this research is purposed to study the effect of resistance spot welding parameters on copper and brass alloy. The copper and brass welded by resistance spot welding technique under varied welding currents and applied loads has been investigated. A nugget measurement looked at the influence of loads (60 N, 65 N, 70 N and 75 N) and weld currents (5.50 kA, 6.00 kA and 6.50 kA) on both fusion area and internal porosity. Nugget diameter increased at low and high-level of welding current, but significantly restricted to a maximum value at intermediate level of welding. Furthermore, copper joints revealed more oxide formation and crack development, while brass joints revealed some pores and excess penetration in the fusion area. Thus, the weld currents were increased up to 8.00 kA, 8.50 kA and 8.90 kA, while applied load parameters were kept constant at 60 N, 65 N, 70 N and 75 N to which taken as optimised values to improve the weld joined. The mechanical properties and microstructure of these welded copper and brass was detailed. Specimens joined at higher welding current yielded higher tensile-shear strength results than those joined at lowest welding current. Failure modes are detailed by observing weld fracture surfaces. A correlation between base metal and fusion zone hardness is produced. The hardness of brass joints gave the highest hardness values due to grains refinement resulted from the weld nugget zone and this was followed

by HAZ and original base metal. While copper joints revealed the weld nugget gives the lowest hardness values than the original base metal due to annealing softening was dominant caused coarsening grain structures.

## **CHAPTER 1**

### **INTRODUCTION**

#### **1.1 Resistance spot welding in general**

Resistance spot welding (RSW) is the most commonly used method for joining sheet metals. Spot welding is a widely used in joining process for fabricating sheet metal assemblies such as automobiles, truck cabins, rail vehicles and home applications due to its advantages in welding efficiency and suitability for automation (Hou et al., 2007). For example, modern auto-body assembly needs 7000 to 12, 000 spots of welding depending to the size of a car (Huh and Kang, 1997). Resistance spot welding is also suitable for small batch production because the method is flexible, equipment simple and the welding process is easy to control (Rautaruukki, 2009).

Work stages in resistance spot welding are very fast. Resistance welding methods are inexpensive and efficient, which has made them highly popular in the making of sheet joints. Resistance spot welding is a process in which faying surfaces are joined in one or more spots by resistance to the flow of electric current through worksheets, which are held together under force by electrodes. The contacting surfaces in the region of current concentration are heated by a short-time pulse of low voltage, high-amperage current to form a fused nugget of weld metal. When the flow of current ceases, the electrode force is maintained while the weld metal rapidly



cools and solidifies. The electrodes are retracted after each weld, which usually is completed in a fraction of a second (Neville and Bristish, 1993).

There are three stages in making spot weld are illustrated in Figure 1.1. First the electrodes press the welded worksheets together and decrease the transfer resistance of worksheets between the electrodes, which allows directing welding current through the desired route. Then, the welding current is connected after termination of the squeeze time. Welding current produces heat at the faying surfaces and thus creates a weld pool between the worksheets. This is followed by the third or hold time, which welding current is switch off as the weld time ends, but electrode force still presses the worksheets together and electrodes cool the weld down. The hold time forges the worksheets while it is cooling, where the weld pool must solidify and must achieve sufficient strength properties during the hold time (Rautaruukki, 2009).

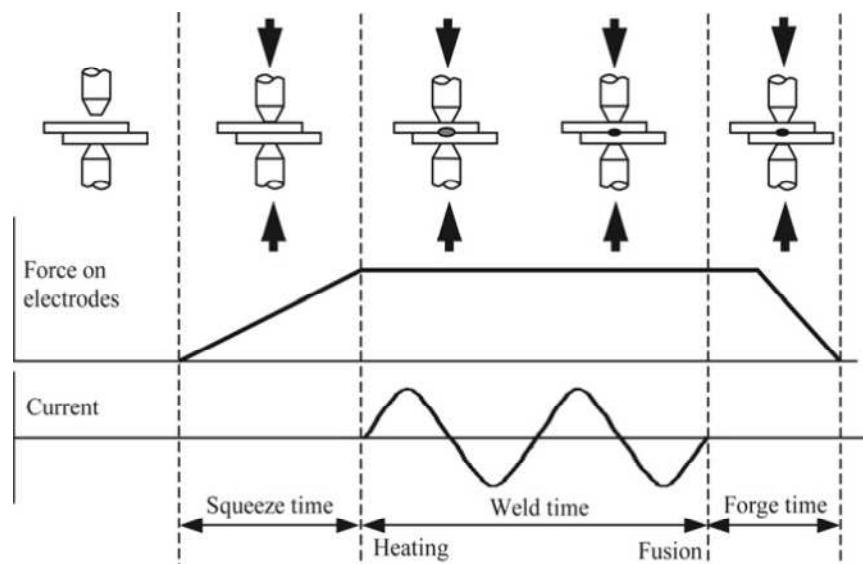


Figure 1.1 Typical spot welding cycle (Kahraman, 2007)

The key variables that must be controlled to achieve consistently acceptable welds are the welding energy used to generate heat, the amount of time that the energy is applied, the physical weld force that is applied and the quality of the materials being joined, including metallurgic properties, resistance, thickness, configuration and coatings ([www.mddionline.com](http://www.mddionline.com))

Factors affecting the amount of heat being generated by a given weld current for a unit of time are; the electrical resistance of the materials being welded, the electrical resistance of the electrode materials, the contact resistance between the parts as determined by surface conditions, scale, welding pressure and the contact resistance between the electrodes and parts as determined by surface conditions, area of electrode contact and welding pressure. In most resistance welding machine, welding current is adjusted as a percentage of the nominal power of the machine, although in some equipment adjustment is made by changing the transformation ratio of the welding transformer (Rautaruukki, 2009).

Mechanical testing is an important aspect of weld ability study. Such testing is either for revealing important welds characteristics, such as weld nugget diameter or weld button size, or for obtaining and evaluating the quantitative measures of weld's strength. Mechanical testing of a weldment can be static or dynamic test and among the static test, tension shear or tensile shear testing is commonly used in determining weld strength or the tensile strength of the welded joints because it is easy to conduct the test and the specimens for the test is simple in fabrication.

## 1.2 Problem statement

The resistance spot welding process is a very useful way of joining galvanised steels sheets, cast iron, nickel, aluminium and others. In the past, steel is the major material encompassing over 70% of all joining materials in resistance spot welding (Ta-chien, 2003). Most studies in RSW method were focus on selected materials and little information is available regarding the response and behaviour of copper and copper alloy.

Thus, in this research, pure copper and brass (Cu-Zn) alloy were chosen as a base material for joining due to these alloys are typically more difficult to be resistance spot welded. Although copper and copper alloys can be joined by most of the commonly used methods such as gas welding, arc welding, resistance welding, brazing and soldering, the joining of copper is usually difficult by conventional fusion welding methods because copper has a thermal diffusivity of about 401 W/mK, which is almost the highest among all the metallic materials. During welding, much higher heat input is required due to the rapid heat dissipation into the worksheets and the welding speeds are therefore quite low. In addition, the serious oxidation at melting temperature and the thermal crack in the joint are also a stubborn problem and will inevitably deteriorate the mechanical properties of the copper weld (Lee et al., 2003). In addition, different material may show the different effects to the nugget diameter. Copper and brass alloy were chosen in term of its electrical resistivity, thermal conductivity and melting points and these properties would affect the physical and mechanical properties.

On the other hand, extensive research and development work has been carried out on the effects of welding parameters such as welding current, welding time, electrode force, etc. However, most of this work is limited to sheet metals of similar joining of copper-copper sheets and brass-brass sheets by RSW method. The determination of appropriate welding parameters for spot welding is a very complex issue. The welding parameters play an important role on the quality of weld. In addition, controlling a small change of one parameter will affect all the other parameters. Thus, welding current and applied welding load (electrode force) was chosen depends on the material to be welded. In addition, the parameters were selected for relatively thick sheet of copper (0.5 mm thickness) and brass (1.0 mm thickness) used. One problem, though, is that the size of the contact surface will increase during welding. To keep the same conditions, the electrode force needs to be gradually increased. As it is rather difficult to change the electrode force in the same rate as the electrodes are “mushroomed”, usually an average value is chosen (Aslanlar, 2006). However, more work is required in order to understand the effects of RSW parameters on these materials before further implementation can occur.

The aim of this research is to study the effect of RSW parameters on similar joining of copper-copper sheets and brass-brass sheets, also with different thickness. Nugget characteristics, weld nugget sizes, peel off, tensile-shear strength, hardness and metallographic evaluations were considered and each of them has been investigated in details.

### **1.3 Research objectives**

The main focus of the research:

- i. To study the effect of RSW parameters on similar joining of copper-copper sheets and brass-brass sheets metal and their welding performance.
- ii. To study the relationship between welding currents and applied welding load to the nugget diameter and their nugget characteristics for each welded specimens.
- iii. To examine the effect of welding parameters on hardness test and microstructural evaluations on the base metal (BM), heat affected zone (HAZ) and nugget area.
- iv. To analyze the shear-strength of the tensile test properties, the fracture surface and impact performance of spot welded specimens.

### **1.4 Scopes**

In this research, resistance spot welding method was used to study the effect of welding parameters on similar joining of copper-copper sheets and brass-brass sheets metal. Various welding parameters were applied to the specimens. Physical and mechanical properties, microstructural characterization and nugget characteristics with different nugget diameter were evaluated. Three different mechanical testing were conducted, which are peel off test, hardness test and tensile test. Figure 1.2 illustrates the scope in this research.

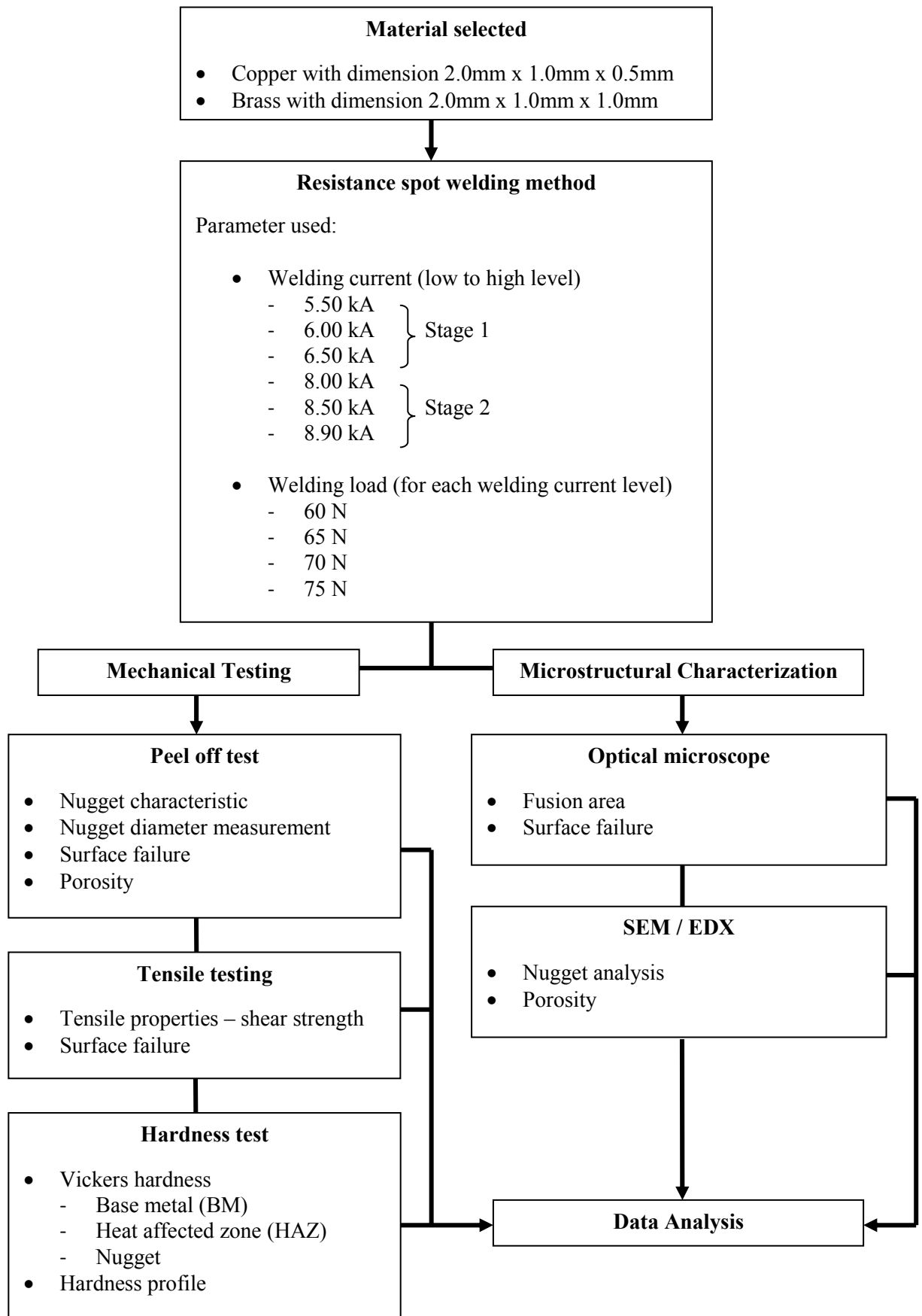


Figure 1.2 Schematic representations of the whole experimental procedures

## **CHAPTER 2**

### **LITERATURE REVIEW**

#### **2.1 Resistance spot welding (RSW)**

Spot welding is one of a group of resistance welding processes that involve the joining of two or more metal parts together in localise area by the application of heat and pressure. The resistance involves electrode and sheet bulk resistances as well as electrode-sheet and sheet-sheet contact resistances.

Spot welding produces single spot like welds, which are called nugget. The spot weld nugget is formed when the interface of the weld joint is heated due to the resistance of the joint surfaces to electrical currents flows. Welding current is directed to the specimens through electrodes, which hold the part to be welded in close contact before, during and after welding. The welding current depends on the material to be welded and specimen thickness. Spot welding also can be used for joining several metallic materials and sheets of different thickness together without large deformation (Rautaruukki, 2009).

The process is used for joining sheet materials and uses shaped copper alloy electrodes to apply pressure and the electrical current flows through the work pieces. Heat is developed mainly at the interface between two sheets, eventually causing the materials being welded to melt, forming a molten pool, a weld nugget. The size and shape of the individually formed welds are limited primarily by the size and contour

of the electrodes faces. Figure 2.1 shows the micro spot welder machines and the spot weld illustration.

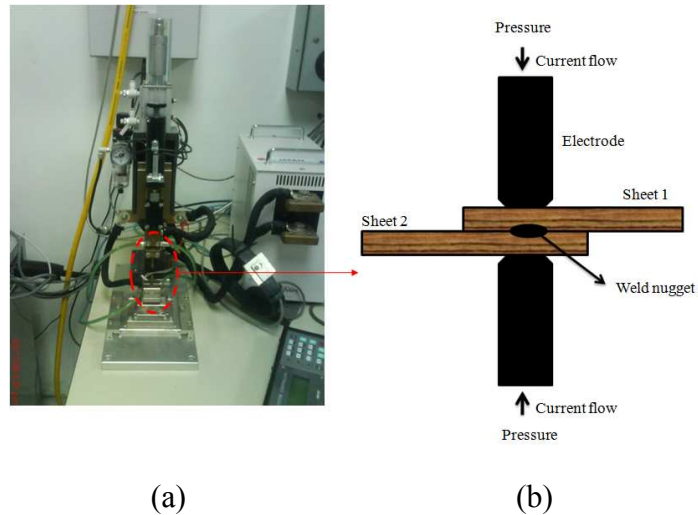


Figure 2.1 Schematic figures of (a) micro spot welder machines and (b) the spot weld illustration

## 2.2 Principle of operation resistance spot welding

The heat required for any resistance spot welding process is produced by the resistance offered to the passage of an electric current through the worksheets. Since the electrical resistance of metals is low, high welding currents are required to develop the necessary welding heat. Typically the currents are in the range of 1000's of amps, while the voltage is at the level of a few volts only.

The rate of heat generation depends upon the flow of current, in amperes, through the resistance offered by the materials. Other electrical factors, such as voltage, frequency and power factor, enter into consideration only with respects to their uniformity. They affect only the value of the current.



According to Ohm's law:

$$I = \frac{E}{R} \quad (2.1)$$

Where  $I$  is the current,  $E$  is voltage drop across the electrodes and  $R$  is the resistance through the metal.  $R$  is the summation of the contact resistance and the resistance of the work to be welded. Therefore, for a given value of  $R$ , the magnitude of  $I$  is determined by  $E$ . Current to the primary of the transformer is controlled which determines the current delivered to a weld of a given resistance. The principle of resistance spot welding is the Joule's heating law, where the heat is generated depending on three basic factors. It can be expressed by equation:

$$Q = I^2 R t \quad (2.2)$$

Where  $Q$  is the heat generated (Joule),  $I$  is the current (amperes),  $R$  is the resistance (ohms) of the base metals and the contact interfaces and  $t$  is the duration of current flow (seconds). From the equation, it can be shown that the current, resistance and time are key parameters for heat generation and hence the quality of the weld.

### **2.2.1 Welding current**

The welding current is the most important parameter, in order to form a nugget between two metal sheets. A larger amount of heat must transmit to the spot in very short period time. Equation 2.2 shows the welding current has more influence than resistance,  $R$  or time,  $t$ , since it has a square power influence. On the other

words, if current is doubled, the heat amount will be equal to four times of the previous value (Guangqian, 2007).

To create the heat, a very high alternative current (AC) or direct current (DC), usually thousands of amperes must be applied. The heat generated depends on the electrical resistance and thermal conductivity of the metal and the time that the current is applied (Guangqian, 2007). The sizes of the weld nugget increase rapidly with increasing welding current, but too high current will results in expulsions and electrode deteriorations.

For example, studied on weldability of thin sheet metals during small-scale resistance spot welding using an alternating-current power supply by Zhou et al. (2000) who figured out the welding current (kA) values for 0.4 mm diameter nugget, weld metal expulsion (WME) and electrode-sheet sticking (ESS) for sheet metals of brass and copper as shown in Table 2.1, which indicated that the welding current having the strongest effect.

Table 2.1 Welding current (kA) for 0.4 mm diameter nugget, WME and ESS  
(Zhou et al., 2000)

Sheet metals	Electrodes	Minimum	Expulsion	Sticking	Suggested range
Brass	Class 2	1.6	2.0	2.6	1.6 - 2.6
	Class 14	1.2	>1.8	~1.4	1.2 - 1.4
Cu	Class 2	≥3.5	3.8	2.8	-
	Class 14	≥2.2	-	2.0	-

\* The minimum current is determined to produce 0.4mm diameter of weld nuggets. Electrode force is 4.5 kg and weld time is 8 cycles

### **2.2.2 Welding force (electrode force)**

The force is one of the main parameters. The influence of force on the quality of the spot welds is important. The purpose of the electrode force is to squeeze the metal sheets to be joined together. The force supplied to the work to be welded, the method of application and the inertia of the moving parts, will greatly influence the quality of the spot weld. It is known that the bearing capability of joints will decrease under too large or too small electrode force (Ao et al., 2008).

However, the force must not be too large as might cause others problems. It presses the metal sheets to be welded together and restricts the passage of current to this area. It also reduces the formation of porosity and cracks in the welded area. A smaller force maintains a low value of contact resistance between the welding tips and sheets to be welded, reducing the tendency of sticking or alloying of the electrodes to materials being welded.

### **2.2.3 Welding time (welding cycles)**

Welding time is the time during which welding current applied to the sheets metal. The heat generation is directly proportional to the welding time. The time is expressed in cycles. The weld time is measured and adjusted in cycles of line voltage as are all timing functions. One cycle is 1/50 of a second in a 50 Hz power system.

In a real environment, when the heat is transferred from the weld zone to the metal sheets, a portion of heat will be lost to the surrounding environment, the

amount of lost is proportional to the welding time, to reduce heat lost and improve welding efficiency, welding applications usually adopt short welding time with high current combination to control the welding machine (Guangqian, 2007).

Resistance spot welding depends on the resistance of the base metal and the amount of current flowing to produce the heat necessary to make the spot weld. To make good resistance spot welds, it is necessary to have close control of the time the current is flowing.

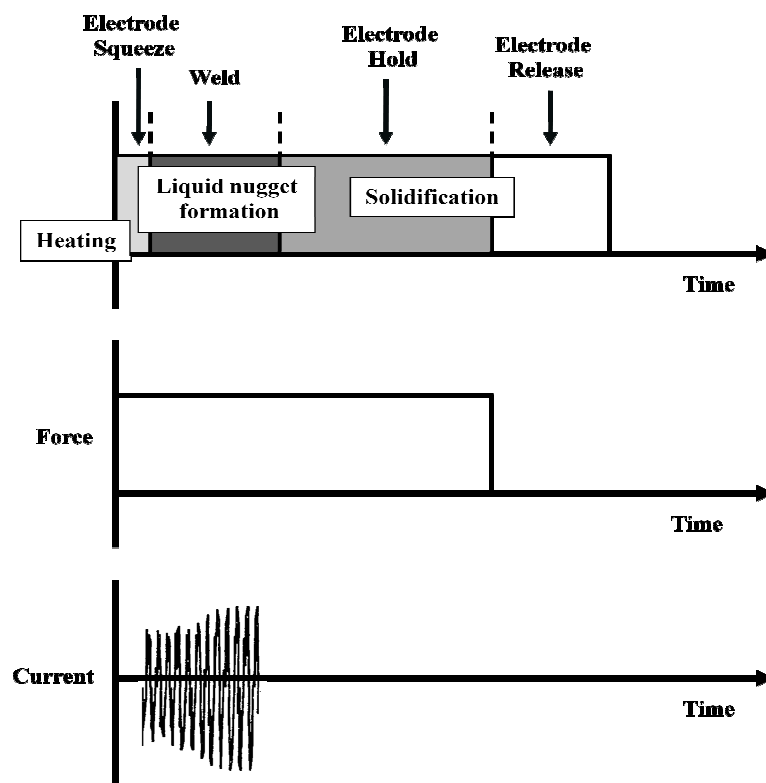


Figure 2.2 Four stage of spot welding process and weld nugget formation (Michelle, 1992)

A spot welding process normally includes four stages which are schematically illustrated in Figure 2.2. During process, the worksheets are squeezed together by a pair of electrodes. Then, electrical current flows through sheet metal. Since the electrical resistance at sheet to sheet (faying surface) is high at the beginning of the weld stage and the heat concentrates around the surface. When the temperature at the faying surface exceeds the melting point of metal, a molten nugget forms at the surface and grows. After the current terminates, the nugget cools down and consolidates, forming a solid spot joint. The weld stage is the most important to weld nugget formation and the hold stage is also important to the solidification of liquid nuggets.

### **2.3 Properties and characteristics of copper and copper alloys**

Copper and copper alloys have been used to make a very wide variety of products that depends on their usefulness on combinations of such properties, strength, ductility, and hardness and corrosion resistance. Copper and copper alloys are classified according to a designation system administered by the Copper Development Association (CDA). In this system, numbers from C100 through C799 designate wrought alloys and numbers from C800 to C999 cast alloys. Within these two main classes, the system is divided into groups and subgroup (William, 2004).

Table 2.2 Copper and copper alloys are classified according to a designation system administered by the Copper Development Association (CDA)

<b>Wrought alloys</b>	
C1xx	Coppers <sup>1</sup> and high-copper alloys <sup>2</sup>
C2xx	Copper-zinc alloys (brasses)
C3xx	Copper-zinc-lead alloys (leaded brasses)
C4xx	Copper-zinc-tin alloys (tin brasses)
C5xx	Copper-tin alloys (phosphors bronzes)
C6xx	Copper-aluminium alloys (aluminium bronzes), copper-silicon alloys (silicon bronzes) and miscellaneous copper-zinc alloys
C7xx	Copper-nickel and copper-nickel-zinc alloys (nickel silvers)
<b>Cast alloys</b>	
C8xx	Cast copper, cast high-copper alloys, the cast brasses of various types, cast manganese-bronze alloys and cast copper-zinc-silicon alloys
C9xx	Cast copper-tin alloys, copper-tin-lead alloys, copper-tin-nickel alloys, copper-aluminium-iron alloys and copper-nickel-iron and copper-nickel-zinc alloys

<sup>1</sup> "Coppers" have a minimum copper content of 99.3% or higher

<sup>2</sup> High-copper alloys have less than 99.3% Cu, but more than 96% and do not fit into the other-copper alloy group

### 2.3.1 Copper

The basic properties of copper alloys are largely influenced by the properties of copper itself. These are high thermal conductivity, excellent ductility and toughness over a wide range of temperatures and excellent corrosion resistance in many different environments. All of the three qualities above are directly related to the structure and behaviour of copper's structure on an atomic scale. The copper atom is quite similar to an atom of gold or silver, which together with copper make up group in the periodic table of the elements. Solid copper can be described as the arrangement of copper atom in a face-centered-cubic (FCC) configuration.

There was only limited success in RSW of copper. The reasons are that the power required is very high due to very high thermal conductivity and low electrical resistance of copper and the high heat generation causes severe electrode-sheet sticking or even welding between the copper sheets and electrodes. Copper is one of those metals that are the least suitable for RSW because of its low electrical resistivity and high thermal conductivity. There is now an increased demand for a copper based material having both high electrical conductivity and high mechanical strength at elevated temperatures.

### **2.3.2 Brass (Cu-Zn) alloy**

Brass alloy widely used as engineering materials in industry because of their high strength, high corrosion resistance, and high electrical and thermal conductivity. They are easily shaped and they possess nice appearance. Brass alloy, as known are copper (Cu) and zinc (Zn) alloys. The copper-zinc brasses consist of a series of alloys of copper with up to about 40% Zn. As the percentage of zinc changes, the properties of the Cu-Zn alloys change also. Copper-zinc brasses containing additional elements such as tin, aluminium, silicon, manganese, nickel and lead are referred to as “alloy brasses”. The alloying additions, which rarely exceed about 4%, improve some of the properties of the strength Cu-Zn brasses so they can be used for other applications (William, 2004).

The main problem with these alloys is the evaporation of zinc during the welding process. After welding, the weld metal becomes porous. Moreover, since the amount of zinc in the alloy is reduced due to evaporation, the brass material loses the

physical and chemical properties which it normally possesses. Studies on weldability of brass materials are very few. There is very little information concerning the weldability of brass materials in the literature and general definitions are often seen.

Brasses are used in applications such as blanking, coining, drawing, piercing, springs, fire extinguishers, lamp fixtures, flexible hose and the base for gold plate. Brasses have excellent castability and a good combination of strength and corrosion resistance.

#### **2.3.2.1 Structure with Cu-Zn phase diagram**

The phase diagram for the copper-zinc system is shown in Figure 2.3. Zinc has extensive solid solubility in copper and forms  $\alpha$ -solid solutions with up to 39% Zn at 456°C. With increasing zinc content, a second solid solution of zinc in copper is formed which is designated the  $\beta$  phase. The  $\alpha$ -solid has the FCC structure. The  $\beta$  phase has the BCC crystal structure and transforms upon cooling through the 468°C to 456°C temperature range from a disordered  $\beta$  phase structure to an ordered  $\beta'$  structure. With more than about 50% Zn, the  $\gamma$ -phase solid solution forms, this has a complex structure and which is very brittle. Copper- zinc alloys containing the brittle  $\gamma$ -phase are of little engineering use (William, 2004).



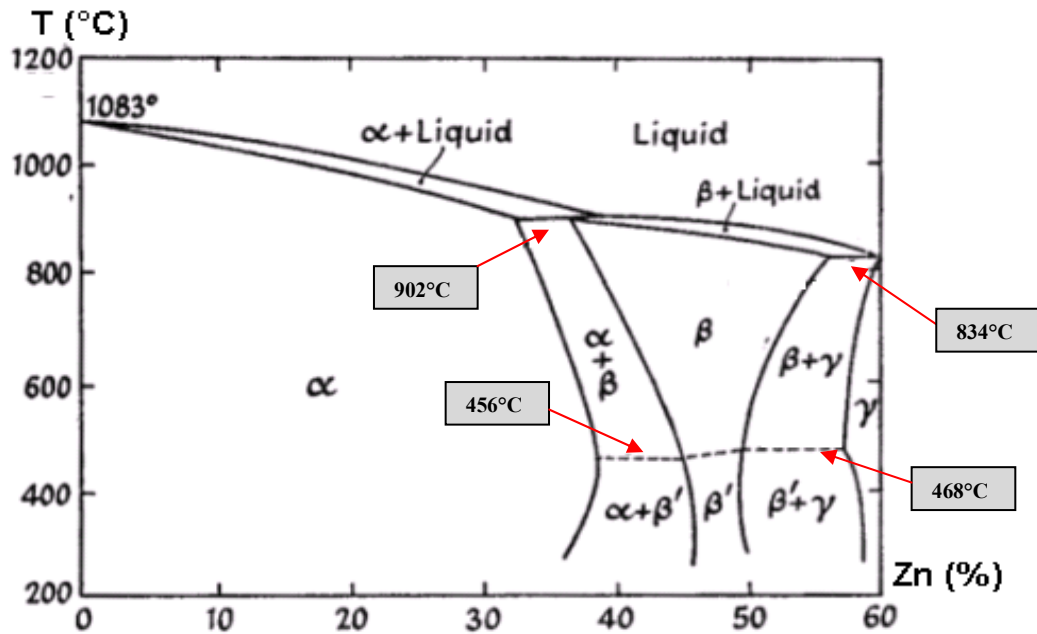


Figure 2.3 Schematic figure of constitutional phase diagram of the Cu-Zn alloy  
(www.keytometals.com)

The addition of zinc to copper results in the formation of a series of solid solutions which, in accordance with usual practice, are referred to in order of diminishing copper contents as the  $\alpha$ ,  $\beta$ ,  $\gamma$ , etc constituents. The diagram may be summarized as follows:

Table 2.3 Table of further changes in percentage composition of copper and zinc  
(www.keytometals.com)

Percentage composition		Constituent just below the freezing point	Constituent after slow cooling to 400°C
Copper	Zinc		
100 to 67.5	0 to 32.5	$\alpha$	$\alpha$
67.5 to 63	32.5 to 37	$\alpha + \beta$	$\alpha$
63 to 61	37 to 39	$\beta$	$\alpha$
61 to 55.5	39 to 45.5	$\beta$	$\alpha + \beta'$
55.5 to 50	45.5 to 50	$\beta$	$\beta'$
50 to 43.5	50 to 56.5	$\beta$	$\beta' + \gamma$
43.5 to 41	56.5 to 59	$\beta$	$\beta' + \gamma$

The important alloys of copper and zinc from an industrial point of view are the brasses comprised within certain limits of zinc content. If the alloy composition is exactly equal to peritectic composition,  $\alpha$ -phase and liquid phase are consumed completely in the peritectic transformation (peritectic reaction).

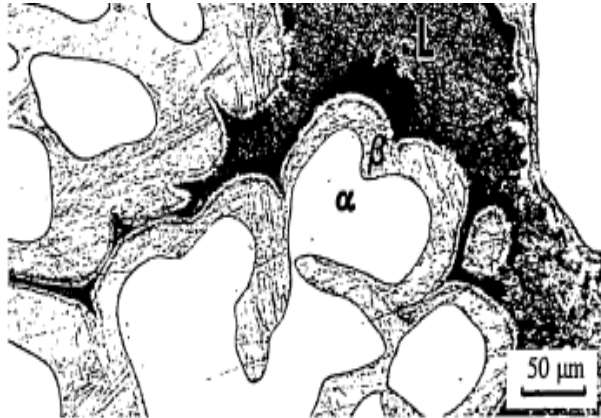


Figure 2.4 Classic microstructure of peritectic alloy, showing rim of  $\beta$ -phase separating primary  $\alpha$ -phase from (darker) former liquid phase, in Cu-20wt-% Sn (Kerr and Kurz, 1996)

Figure 2.4 shows an example microstructure of peritectic alloy, showing rim of  $\beta$ -phase separating primary  $\alpha$ -phase from (darker) former liquid phase, in Cu-20 wt-% Sn. In other words, the peritectic phase tends to form a rim around the primary solid  $\alpha$ -phase (Kerr and Kurz, 1996).

### 2.3.2.2 Phase transformation

An example of a phase diagram with peritectic transformation is shown in Figure 2.5. Consider solidification of an alloy with concentration  $C$ . When the alloy temperature is higher than  $T_L$ , single liquid phase exists (point  $M$  on the diagram). When the temperature reaches the value  $T_L$  (point  $M_1$  on the liquidus curve)

solidification starts. According to solidus curve (point  $N_1$ ) the first solid crystals (primary crystals) of the  $\alpha$ -phase have composition  $C_1$ .

Further cooling of the alloy causes changing of the liquid phase composition according to the liquidus curve and when the alloy temperature reaches a certain intermediate value  $T$  (position  $M_T$ ), liquid phase of composition  $C_y$  and solid  $\alpha$ -phase of composition  $C_x$  are in equilibrium. At the temperature equal to  $T_P$  (peritectic temperature) formation of the  $\alpha$ -phase crystals stops and the remaining liquid phase, having composition  $C_L$  reacts with  $\alpha$ -phase crystals, forming  $\beta$ -phase of composition  $C_P$  (peritectic phase transformation). At this temperature remaining  $\alpha$ -phase crystals have composition  $C_\alpha$  and all crystals of  $\beta$ -phase have composition  $C_P$  (peritectic composition).

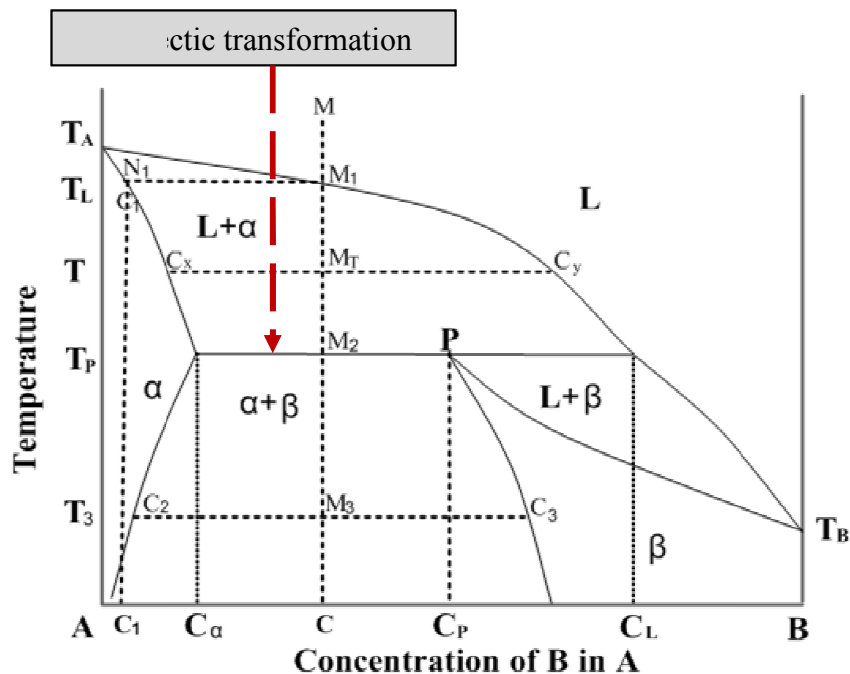


Figure 2.5 Example of a phase diagram with peritectic transformation  
(www.substech.com)

## 2.4 Nugget formation and their characteristics

The formation, size and growth rate of weld depend on the welding parameters used. During the RSW process, resistance at the faying surface generates heat which can cause peak temperatures to exceed liquidus. The nugget in a properly formed spot weld is round or oval in shape. Figure 2.6 shows an example of micrograph of the spot welded region; (a) weld nugget, (b) heat affected zone (HAZ), where the welding process has affected the materials properties and (c) base metal.

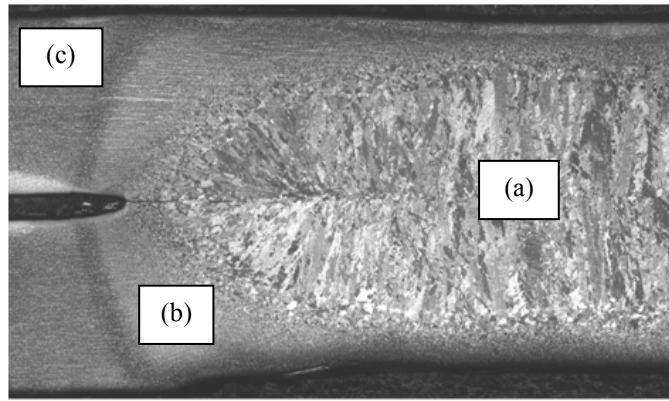


Figure 2.6 Micrograph of the spot welded region, (a) weld nugget, (b) heat affected zone (HAZ) and (c) base metal (Khan, 2007)

The HAZ is the portion of the material which has not been melted, but whose microstructure and mechanical properties are altered by the heat of welding. The nature of the thermal cycle at any position within the HAZ can be characterized by two parameters, the peak temperature  $T_p$  and the time period  $\Delta t_{8-5}$ . Both of these parameters increase with the heat input  $q$ :

$$T_p \propto \frac{q}{r} \quad (2.3)$$

$$\Delta t_{8-5} \propto q^n \quad (2.4)$$

where  $r$  is the distance from the fusion boundary and  $n$  has a value (1 or 2) which depends on whether the component being welded is thick compared with the size of the weld bead (Weisman, 1981).

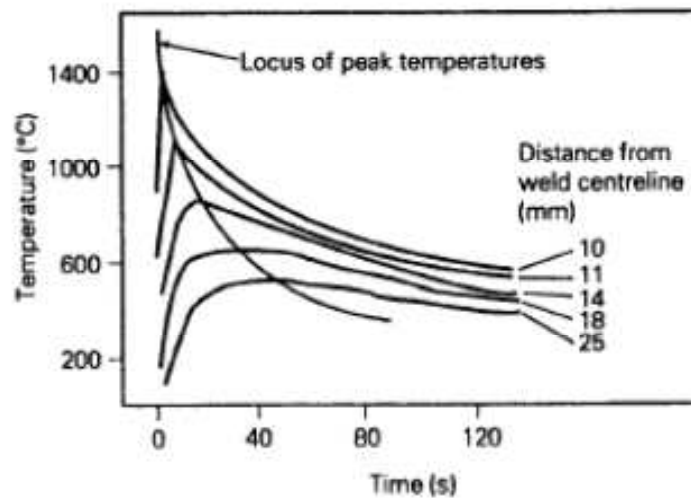


Figure 2.7 Temperature-time curves representing typical thermal cycles experienced in the HAZ of a weld (Weisman, 1981)

Effect of different weld current used for joining on the microstructure of weldments was studied by Dursun (2009). He was reported that the effect of heat input related with weld current on the microstructure of welded materials. It was found that the grain size of weld nugget and HAZ of welded materials were increased by raising the heat input. As seen from Figure 2.8, an increase in welding current from (a) 4 kA to (b) 7 kA and (c) 9 kA caused coarsening of structure. This figure illustrates a difference in microstructure of weld nugget due to different welding current.

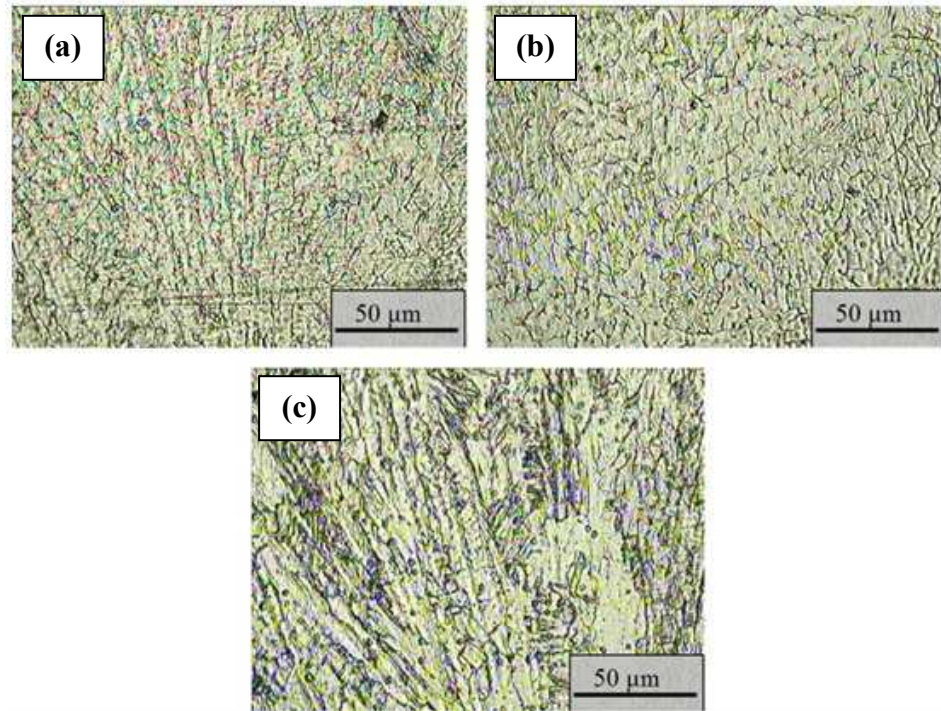


Figure 2.8 Samples, welded in atmosphere and then cooled in atmosphere, show microstructures of weld nugget coarsening by increasing weld current from (a) 4 kA to (b) 7 kA and (c) 9 kA (Dursun, 2008)

Harlin et al. (2003) reported on the studies of weld growth mechanism of resistance spot welds in zinc coated steel. Studies shows that the zinc coated steel melts at the faying surface and increasing the electrode force had major effects on the location of heat development and weld nugget formation. Furthermore, the increase electrode force provided improved consolidation of the molten weld pool such that internal weld porosity was reduced. Variation in electrode force indicated flexibility in the selection of welding conditions to produce an acceptable weld quality. Figure 2.9 shows an examples of typical micrographs illustrating the location of weld nugget, whilst the location of initial heat development and weld nugget formation in the coated stack was different to that in the uncoated variant, the weld quality was unaffected.

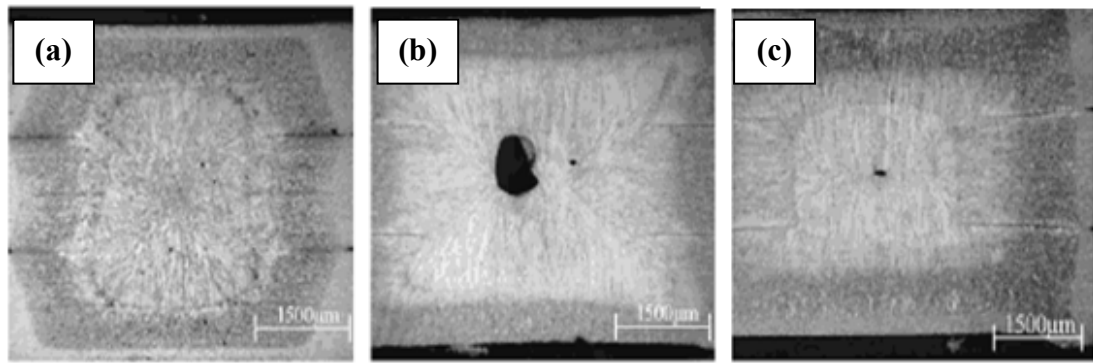


Figure 2.9 Typical micrographs illustrating the location of weld nugget after (a) 9 cycles of current flow in the uncoated stack with an electrode force of 2.1 kN, (b) 10 cycles of current flow in the coated stack with an electrode force of 2.1 kN, and (c) 16 cycles of current flow in the coated stack with an electrode force of 6.0 kN (Harlin et al., 2003)

Rautaruukki (2009) studied that the minimum acceptable diameter of weld nugget is considered to be  $3.5\sqrt{t}$ , where  $t$  is the thickness. Weld nugget which have a smaller diameter do not have sufficient penetration and the size is not enough to bear the calculation loads. A recommended weld diameter is  $5\sqrt{t}$ . This value is usually achieved slightly under the splash limit, where the weld nugget growth is stabilised and small variation in the welding current or workpiece surface quality do not significantly change the size of the weld.

Figure 2.10 shows how the weld nugget diameter increases rapidly at the beginning of the process, and the growth slows down at the end of the curve. This is because the nugget is too large for the electrodes to hold the weld pool between the welded sheets, which causes a burst of molten metal (Rautaruukki, 2009).

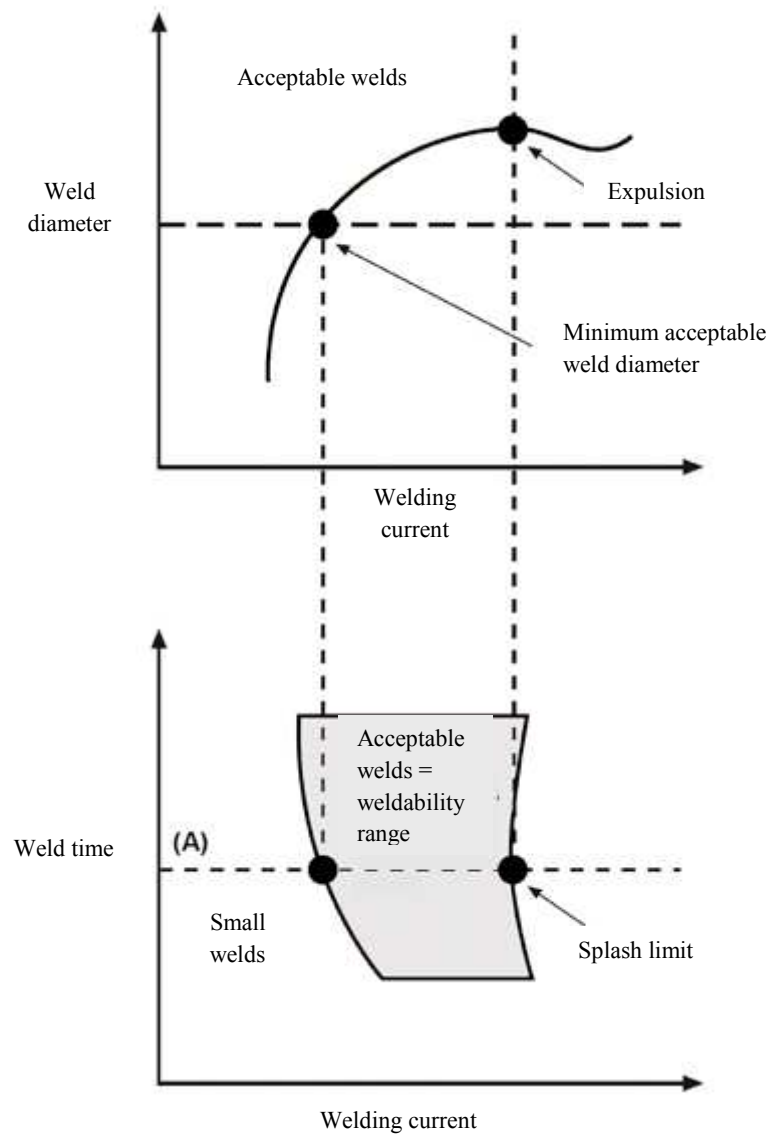


Figure 2.10 Weld nugget growth curve and weldability range (Rautaruukkki, 2009)

Numerical study of nugget formation in resistance spot welding by Mohsen and Hamed (2008) shows that as electrode force increased, contact radius increased. It can be seen in Figure 2.11 (a) and due to Joule' heat effect, as contact area enlarged, the generated heat at interfaces reduced and nugget size decreased as shown in Figure 2.11 (b). They noted that with reduction of force, for increasing nugget size, expulsion phenomenon occurs.